Atomic electron affinities and the role of symmetry between electron addition and subtraction in a corrected Koopmans approach

A. M. Teale,*[a,b] F. De Proft,[c] P. Geerlings,[c] and D. J. Tozer[d]

Received Xth XXXXXXXXXX 20XX, Accepted Xth XXXXXXXXX 20XX
First published on the web Xth XXXXXXXXXX 200X
DOI: 10.1039/b000000x

The essential aspects of zero-temperature grand-canonical ensemble density-functional theory are reviewed in the context of spin-density-functional theory and are used to highlight the assumption of symmetry between electron addition and subtraction that underlies the corrected Koopmans approach of Tozer and De Proft (TDP) for computing electron affinities. The issue of symmetry is then investigated in a systematic study of atomic electron affinities, comparing TDP affinities with those from a conventional Koopmans evaluation and electronic energy differences. Although it cannot compete with affinities determined from energy differences, the TDP expression yields results that are a significant improvement over those from the conventional Koopmans expression. Key insight into the results from both expressions is provided by an analysis of plots of the electronic energy as a function of the number of electrons, which highlight the extent of symmetry between addition and subtraction. The accuracy of the TDP affinities is closely related to the nature of the orbitals involved in the electron addition and subtraction, being particularly poor in cases where there is a change in principal quantum number, but relatively accurate within a single manifold of orbitals. The analysis is then extended to a consideration of the ground state Mulliken electronegativity and chemical hardness. The findings further emphasize the key role of symmetry in determining the quality of the results.

1 Introduction

The calculation of electron affinities remains a challenging and controversial issue for density-functional calculations [1–9]. In particular, local and semi-local approximate exchange–correlation functionals typically provide a poor description of anionic species due to large self-interaction errors (SIEs). A key perspective in the understanding of SIEs and their influence on calculated electron affinities comes from studying the variation in electronic energy E as a function of the average particle number M using zero-temperature grand-canonical ensemble density-functional theory (ZTGC-EDFT) [10–15] in the context of spin-density functional theory [16–19].

It has been known since the pioneering work of Perdew et al. [11] that the exact ZTGC-EDFT electronic energy, as a function of M, comprises a series of straight line segments with derivative discontinuities at the points where M is integer. However, when calculations are performed using typical (semi-) local density functional approximations a convex rather than linear behaviour is usually observed between the integers and this deviation from linearity has been termed many electron self-interaction error (MSIE) [16,18,19] or delocalization error [20–24], the latter terminology applying only to the case of convex behaviour between integer particle numbers. Traditionally, SIEs were understood in terms of one-electron self-interaction terms arising in the Kohn–Sham equations due to an incomplete screening of the classical Coulomb self-interaction by approximate exchange–correlation functionals. However, even for methods that by construction are free of these one-electron SIEs, significant MSIEs can still remain [16,18,19]. These MSIEs have a profound impact on the ways in which (semi-) local approximate functionals may be used to determine electron affinities, particularly when using relations derived for the frontier molecular orbitals.

A further complicating issue when using DFT to calculate affinities with approximate exchange–correlation functionals is the use of localized atom centred basis sets. To some extent the problems arising from MSIE may be exacerbated by artificial binding effects if the basis sets chosen do not contain sufficiently diffuse functions. In some circumstances this effect may be exploited to study, for example, temporary anions with negative electron affinities [25], which do not bind the excess electron. However, in general it can lead to energies for species with $M > Z$ that are constrained to be too high by the compact nature of the basis set employed, even if the excess electron is weakly or partially bound corresponding to a pos-

[a] *School of Chemistry, University of Nottingham, University Park, Nottingham, NG7 2RD, UK. Fax: XX XXXX XXXX; Tel: +44 115 84 68482; E-mail: andrew.teale@nottingham.ac.uk*
[b] *Centre for Theoretical and Computational Chemistry, Department of Chemistry, University of Oslo, P. O. Box 1033, Blindern, N-0315, Oslo, Norway.*
[c] *Eenheid Algemene Chemie (ALGC), Vrije Universiteit Brussel (VUB), Pleinlaan 2, 1050, Brussels, Belgium.*
[d] *Department of Chemistry, Durham University, South Road, Durham, DH1 3LE, UK.*

itive electron affinity in the ground state. Care must therefore be taken when attempting to assess the accuracy of calculations of electron affinities using DFT.

Two natural routes to remedy the shortcomings of approximate functionals in this context have been considered. In the first, one attempts to fundamentally improve the E vs. M behaviour of approximate functionals; substantial recent efforts have been devoted to this task[26–30]. However, many of the proposed solutions to this problem involve proceeding beyond the Kohn–Sham framework to introduce some of the Hartree–Fock-type exchange contribution, often in a range-separated[31] hybrid manner. Whilst effective in improving the E vs. M behaviour, these approximations are typically less computationally expedient than (semi-) local functionals. The alternative route is to seek a correction enabling the calculation of electronic affinities using existing (semi-) local functionals. Along these lines, Tozer and De Proft (TDP) proposed an unconventional expression for the electron affinity[32,33], based on the assumption that the exchange–correlation potentials associated with these functionals average over the potentials associated with approaching the integer particle number, N, from the electron deficient and electron abundant sides. The TDP expression takes the form of a corrected Koopmans' type expression and requires calculations at only the N and $N-1$ particle systems for its evaluation, thereby avoiding many of the controversies associated with DFT calculations on anions.

Electron affinities determined using the TDP expression correlate well with experimental values, both for systems displaying positive affinities and those for which negative values may be observed by electron transmission spectroscopy[32–35]. For systems with positive affinities, the expression is not competitive with a conventional evaluation, which takes the difference between the electronic energies of the neutral and anionic species. However, for systems where the affinity is negative, it circumvents the basis set issues associated with computations on an anion that does not bind the excess electron. Further analysis of the TDP expression by Teale *et al.*[36] emphasized, schematically, the connections between (i) the extent to which the assumption that the exchange–correlation potential averages over the functional derivative discontinuity holds, (ii) Janak's theorem[37] and (iii) the behaviour of the electronic energy calculated at non-integer particle numbers. When the errors in the gradient of the electronic energy with respect to M either side of the integer are of similar magnitude then the TDP expression delivers reasonable accuracy. This may be understood as a symmetry between the errors due to the approximate nature of the functional form under the processes of electron addition and subtraction.

The aim of the present study is to quantify the symmetry between the errors obtained upon electron addition and subtraction, identifying the situations in which the TDP expression may be regarded as a reasonable approximation and those where it is likely to fail. To achieve this we consider a range of atomic species from across the periodic table from lithium to iodine, allowing the systematic study of species with many different electronic configurations and their changes upon electron addition and subtraction. Electron affinities determined using the TDP expression are compared with values from the DFT analogue of Koopmans' theorem and conventional electronic energy differences. We also consider the extent to which the assumptions underlying the TDP expression may be applied to the calculation of other properties key to chemical reactivity, namely the Mulliken electronegativity and molecular hardness. We commence in Section 2 by setting out the essential theory. Results and conclusions are presented in Sections 3 and 4, respectively.

2 Background and Theory

2.1 Essentials of ZTGC-EDFT

Throughout the present work we will make use of the ZTGC-EDFT approach to consider the treatment of systems with fractional particle numbers. The ZTGC-EDFT theory used here follows the initial finite temperature work of Mermin[10] and the pioneering zero-temperature works of Perdew *et al.*[11] and Sham and Schlüter[13]. For a review of the key ideas and their application in the context of spin-density functional theory see the work of Chan[38]. Here we present only the key results from ZTGC ensemble spin-density functional theory relevant to the present work.

In ZTGC-EDFT the system is described in terms of the density operator,

$$\hat{\Gamma} = \sum_{iN} p_{iN} |\Psi_{iN}\rangle\langle\Psi_{iN}|, \qquad p_{iN} \geq 0, \qquad \sum_{iN} p_{iN} = 1 \tag{1}$$

where $|\Psi_{iN}\rangle$ are pure states containing N electrons and p_{iN} are their associated probabilities. The total number of particles in the system is given by $M = \sum_{iN} p_{iN} N$ and may be non-integer. In the context of spin-ensemble density-functional theory the ground-ensemble density $\rho_0 = \rho_0^\alpha + \rho_0^\beta$ is determined by minimization of the grand canonical potential

$$\begin{aligned}\Omega[\rho^\alpha, \rho^\beta] &= \min_{\hat{\Gamma}\to(\rho^\alpha,\rho^\beta)} \mathrm{Tr}[(\hat{H} - \mu^\alpha M^\alpha - \mu^\beta M^\beta)\hat{\Gamma}] \\ &= E[\rho^\alpha, \rho^\beta] - \mu^\alpha M^\alpha - \mu^\beta M^\beta \end{aligned} \tag{2}$$

at fixed external potential $v_{\mathrm{ext}}(\mathbf{r})$ where μ^σ are the σ-spin chemical potentials, and M^σ the average spin-particle numbers.

The ground state energy E_0 is assumed to be a convex function of the average particle number $M = M^\alpha + M^\beta$ and no known experimental counter examples have been found to date[39–41]. The convexity implies that the density operator $\hat{\Gamma}$

interpolates between the $(N^\sigma, N^{\sigma'})$ and $(N^\sigma, N^{\sigma'} \pm 1)$ pure state density matrices for particle numbers $(M^\sigma, M^{\sigma'})$ between $(N^\sigma, N^{\sigma'})$ and $(N^\sigma, N^{\sigma'} \pm 1)$. In general for changes in the spin-particle numbers $N^\alpha \pm \omega^\alpha$, $N^\beta \pm \omega^\beta$ $(0 < (\omega^\alpha + \omega^\beta) < 1)$, the ground state energy is given by

$$\begin{aligned} E_0(N^\alpha \pm \omega^\alpha, N^\beta \pm \omega^\beta) = (1 - \omega^\alpha - \omega^\beta) E_0(N^\alpha, N^\beta) \\ + \omega^\alpha E_0(N^\alpha \pm 1, N^\beta) \\ + \omega^\beta E_0(N^\alpha, N^\beta \pm 1) \end{aligned} \tag{3}$$

where pure state interacting v-representability is assumed at the integers. The ground state energy as a function of particle number then comprises a series of linear segments between integer numbers of electrons, giving rise to derivative discontinuities at the integers[11]. In the present work we shall limit ourselves to the consideration of changes which involve only the addition / removal of a particle with one particular spin between any two integer particle numbers.

The Euler–Lagrange equation associated with the variation of $E[\rho^\alpha, \rho^\beta]$ in Eq. (2) at constant average spin particle numbers M^σ is

$$\left[\frac{\delta E[\rho^\alpha, \rho^\beta]}{\delta \rho^\sigma} - \mu^\sigma \right]_{(\rho_0^\alpha, \rho_0^\beta)} = 0 \tag{4}$$

where the Lagrange multiplier is identified as the spin chemical potential

$$\mu^\sigma = \frac{\partial E_0}{\partial M^\sigma} = \left(\frac{\delta E[\rho^\alpha, \rho^\beta]}{\delta \rho^\sigma} \right)_{(\rho_0^\alpha, \rho_0^\beta)} \tag{5}$$

However, it should be noted that the derivatives in Eq (5) are not uniquely defined for integer values of M. At the integers derivative discontinuities arise in Eq (5) and accompanying functional derivative discontinuities in Eq. (4), see e.g. Refs. 11,38. Here the functional derivative is chosen to be evaluated along the path of ground ensemble-state densities $(\rho_0^\alpha, \rho_0^\beta)$, see Ref. 38 for further discussion.

The spin-chemical potentials obtained by evaluating the partial derivative in Eq (5) with respect to the average spin-particle number on each side of the integer are,

$$\mu^\sigma((N^\alpha, N^\beta) - \omega^\sigma) = -I^\sigma(N^\alpha, N^\beta) \tag{6}$$

$$\mu^\sigma((N^\alpha, N^\beta) + \omega^\sigma) = -A^\sigma(N^\alpha, N^\beta) \tag{7}$$

Since the energy of Eq. (3) comprises a series of straight line segments these derivatives are well defined between integer particle numbers and are consistent with the conventional definitions

$$I^\sigma(N^\alpha, N^\beta) = E_0((N^\alpha, N^\beta) - 1^\sigma) - E_0(N^\alpha, N^\beta) \tag{8}$$

$$A^\sigma(N^\alpha, N^\beta) = E_0(N^\alpha, N^\beta) - E_0((N^\alpha, N^\beta) + 1^\sigma) \tag{9}$$

however, the derivatives are not well defined at the integer values. In fact, at the integer values an order of limits problem arises. Choosing to take the limit $\omega^\sigma \to 0$ before the zero temperature limit gives a chemical potential on integer that corresponds to the ensemble average,

$$\mu^\sigma(N^\alpha, N^\beta) = -\frac{1}{2}[I^\sigma(N^\alpha, N^\beta) + A^\sigma(N^\alpha, N^\beta)] \tag{10}$$

as obtained in Refs. 11,12,14,42. It should be noted however that this result represents only a convenient choice from infinitely many allowable values in the range $I^\sigma \leq \mu^\sigma \leq A^\sigma$ [11,15]. If, for example, one first takes the zero temperature limit and then $\omega^\sigma \to 0$, Eq. (6) is obtained when approaching N from below and Eq. (7) is obtained when approaching N from above.

2.2 Kohn–Sham ZTGC-EDFT

Introducing an auxiliary system of non-interacting electrons with the same spin densities $(\rho_0^\alpha, \rho_0^\beta)$ and chemical potentials (μ^α, μ^β), then the usual decomposition of the electronic energy into non-interacting kinetic (T_s), electron-nuclear (E_ne), classical Coulomb (E_J) and exchange–correlation (E_xc) components gives the alternative Euler–Lagrange equation,

$$\left[\frac{\delta T_\mathrm{s}[\rho^\alpha, \rho^\beta]}{\delta \rho^\sigma} + v_\mathrm{ne}^\sigma + v_\mathrm{J}^\sigma + v_\mathrm{xc}^\sigma[\rho^\alpha, \rho^\beta] - \mu^\sigma \right]_{(\rho_0^\alpha, \rho_0^\beta)} = 0 \tag{11}$$

where the potentials v_ne^σ, v_J^σ and v_xc^σ are the functional derivatives of the corresponding energy components with respect to the σ-spin density. Here the Coulombic contributions to the energy E_ne and E_J have well defined functional derivatives (since they are explicit functionals of the electronic density) for all particle numbers. However, the functional derivatives of the non-interacting kinetic and exchange–correlation energies may be discontinuous.

Using Eqs. (6) and (7) the spin-derivative discontinuity in

E_0 as a function of M may be expressed as

$$\Delta^\sigma = I^\sigma(N^\alpha,N^\beta) - A^\sigma(N^\alpha,N^\beta) \tag{12}$$

$$= \lim_{\omega^\sigma\to 0}[\mu^\sigma((N^\alpha,N^\beta)+\omega^\sigma) - \mu^\sigma((N^\alpha,N^\beta)-\omega^\sigma)] \tag{13}$$

$$= \lim_{\omega^\sigma\to 0}\left[\left.\frac{\delta T_\mathrm{s}[\rho^\alpha,\rho^\beta]}{\rho^\sigma(\mathbf{r})}\right|_{(N^\alpha,N^\beta)+\omega^\sigma} - \left.\frac{\delta T_\mathrm{s}[\rho^\alpha,\rho^\beta]}{\rho^\sigma(\mathbf{r})}\right|_{(N^\alpha,N^\beta)-\omega^\sigma}\right] + \lim_{\omega^\sigma\to 0}\left[\left.\frac{\delta E_\mathrm{xc}[\rho^\alpha,\rho^\beta]}{\rho^\sigma(\mathbf{r})}\right|_{(N^\alpha,N^\beta)+\omega^\sigma} - \left.\frac{\delta E_\mathrm{xc}[\rho^\alpha,\rho^\beta]}{\rho^\sigma(\mathbf{r})}\right|_{(N^\alpha,N^\beta)-\omega^\sigma}\right] \tag{14}$$

$$= (v_{T_\mathrm{s}}^{+,\sigma} - v_{T_\mathrm{s}}^{-,\sigma}) + (v_\mathrm{xc}^{+,\sigma} - v_\mathrm{xc}^{-,\sigma}) \tag{15}$$

$$= \Delta_{T_\mathrm{s}}^\sigma + \Delta_\mathrm{xc}^\sigma \tag{16}$$

where the discontinuity has been separated into contributions from the non-interacting kinetic and exchange–correlation components. The $+/-$ superscripts refer to quantities defined by taking the limit to integer particle number from the electron abundant and deficient sides respectively. The spin-discontinuities here $\Delta^\sigma = I^\sigma(N^\alpha,N^\beta) - A^\sigma(N^\alpha,N^\beta)$ are not necessarily equal to the fundamental band gap $I_0 - A_0$, since the ground state ionization potentials / electron affinities may correspond to processes in which particles of different spin are removed / added. An example of this type will be discussed in Section 3. To make the connection with the fundamental band gap in terms of the chemical potential one can select $\mu^{-,\sigma} = -I_0 = \max(\mu^{-,\alpha},\mu^{-,\beta})$ and $\mu^{+,\sigma} = -A_0 = \min(\mu^{+,\alpha},\mu^{+,\beta})$. Then the fundamental gap (a ground state property) may be written as

$$\Delta_0 = \min_\sigma\left[\lim_{\omega^\sigma\to 0}\mu^\sigma((N^\sigma,N^{\sigma'})+\omega^\sigma)\right] - \max_\sigma\left[\lim_{\omega^\sigma\to 0}\mu^\sigma((N^\sigma,N^{\sigma'})-\omega^\sigma)\right] \tag{17}$$

where σ may differ from σ'. However, since the limiting potentials of different spin are never related by a simple spatial constant no relation of the type in Eq. (16) can be setup.

It has been shown by Sagvolden and Perdew[14] in the context of spin-less DFT that for $M < 2$

$$\Delta_{T_\mathrm{s}} = \varepsilon_\mathrm{LUMO} - \varepsilon_\mathrm{HOMO} \tag{18}$$

where the eigenvalues correspond to a single potential at the integer particle number. However, no rigorous mathematical proof has been presented for systems with more than two electrons. The same authors have also presented arguments in favour of the plausibility of Eq. (18) for $N > 2$. Here we further assume the plausibility of this equation also in its spin-DFT generalization. If this equation is accepted then the exchange–correlation discontinuity is given by

$$\Delta_\mathrm{xc}^\sigma = I^\sigma(N^\alpha,N^\beta) - A^\sigma(N^\alpha,N^\beta) - [\varepsilon_\mathrm{LUMO}^\sigma(N^\alpha,N^\beta) - \varepsilon_\mathrm{HOMO}^\sigma(N^\alpha,N^\beta)] \tag{19}$$

Proceeding in the usual manner one can setup Kohn–Sham equations for ZTGC-EDFT of the type,

$$\left[-\frac{1}{2}\nabla^2 + v_\mathrm{ne}^\sigma + v_\mathrm{J}^\sigma + v_\mathrm{xc}^\sigma\right]\varphi_i^\sigma = \varepsilon_i^\sigma\varphi_i^\sigma \tag{20}$$

The electronic density and non-interacting kinetic energy are then expressed as

$$\rho^\sigma(\mathbf{r}) = \sum_i n_i^\sigma|\varphi_i^\sigma(\mathbf{r})|^2 \tag{21}$$

$$T_\mathrm{s}[\rho^\alpha,\rho^\beta] = \sum_\sigma T_\mathrm{s}^\sigma[\{\varphi_i^\sigma\}] = -\frac{1}{2}\sum_\sigma\sum_i n_i^\sigma\int\varphi_i^\sigma(\mathbf{r})\nabla^2\varphi_i^\sigma(\mathbf{r})\mathrm{d}\mathbf{r} \tag{22}$$

where the solutions correspond to the (M^α,M^β) particle system. The remaining energetic components may be expressed in their usual forms providing they are functionals of the electronic density. For the approximate exchange–correlation functionals of LDA and GGA type this practice is justified, although the specific approximations may not have uniform accuracy for different particle numbers, see the discussion in Ref. 42. In particular, the exchange correlation hole in standard approximate functionals may not be appropriately normalized.

The Kohn–Sham orbitals are fully occupied except for the HOMO which may be fractionally occupied, the occupation numbers n_i^σ being 1 for all levels up to the HOMO. Any standard unrestricted Kohn–Sham code may be modified to solve the Kohn–Sham equations for fractional particle numbers by modifying the construction of the density matrices to correspond to a fixed set of occupation numbers $\{n_i^\sigma\}$ such that $M = \sum_\sigma\sum_i n_i^\sigma$.

In the context of ZTGC-EDFT Kohn–Sham theory, Janak's theorem also applies off integer, where the energy is differentiable, allowing us to make the identifications,

$$\frac{\partial E((N^\alpha,N^\beta)-\omega^\sigma)}{\partial n_{H^-}^\sigma} = \varepsilon_H^{-,\sigma} = -I^\sigma \tag{23}$$

$$\frac{\partial E((N^\alpha,N^\beta)+\omega^\sigma)}{\partial n_{H^+}^\sigma} = \varepsilon_H^{+,\sigma} = -A^\sigma \tag{24}$$

in the case that the exact exchange–correlation functional is employed. For approximate functionals the derivatives of the energy with respect to occupation numbers of the frontier orbital between the integers correspond to the Kohn–Sham eigenvalues, however, the consistency between Eqs. (8), (9) and Eqs. (23), (24) is not guaranteed, unless the behaviour of the energy determined using the Kohn–Sham solutions is linear with particle number. In the absence of this linearity the last equalities with I^σ and A^σ are not justified. The former pair of equations correspond to so called ΔSCF evaluations and rely only on ground state energies at the integer values, whereas the latter rely directly on the quality of the Kohn–Sham eigenvalues and hence depend much more sensitively on the exchange–correlation functional employed, see Section 3 for further discussion.

The functional derivative v_{T_s} may also be explicitly evaluated in the Kohn–Sham framework by multiplying Eq (20) from the left by φ_i^σ, summing over i and comparing with the Euler Eq. (11) to give[43],

$$v^\sigma_{T_s^\sigma} = \frac{\sum_i n_i^\sigma [\frac{1}{2}\varphi_i^\sigma(\mathbf{r})\nabla^2\varphi_i^\sigma(\mathbf{r}) - \varepsilon_i^\sigma(\varphi_i^\sigma)^2(\mathbf{r})]}{\rho^\sigma(\mathbf{r})} + \mu^\sigma \quad (25)$$

This potential has a shape defined by the first term, however, it is shifted by a scalar value equal to the chemical potential of the system. Since the chemical potential at the integer is not uniquely defined, see Eq. (11), then this potential is also only defined in the same manner. This is consistent with the fact that $T_s^\sigma[\{\varphi_i^\sigma\}]$ is not an explicitly differentiable functional of ρ and is expected to display derivative discontinuities as the particle number crosses an integer.

In the present work we will consider the evaluation of the ZTGC-EDFT energy via Eq. (3) using energies calculated with an approximate exchange–correlation functional at integer particle number. We shall also consider the evaluation of the energy obtained with the solutions of the Kohn–Sham Eqs. (20) using the same approximate functional at fractional average particle numbers M. In the exact case the energies should coincide for all values of M. However, (semi-) local functionals contain an inherent inconsistency in this regard since their functional derivatives are smooth and well defined even at the integer. This in turn means that Eqs. (23) and (24) cannot simultaneously hold. It has been argued that the best such functionals can achieve is that the exchange-correlation potential averages over Δ_{xc} as in the open-shell case[12,42].

2.3 Averaging potentials and expressions for the electron affinity

The Janak expressions of Eqs. (23) and (24) are in principle exact due the linearity of Eq (3). By making use of Eq. (23) the exact electronic affinity may also be expressed as

$$A^\sigma = -(\varepsilon_H^{+,\sigma} + \varepsilon_H^{-,\sigma} + I^\sigma) \quad (26)$$

where the last two terms trivially cancel for an exact functional.

The spin generalisation of the TDP expression[32] for use with local (LDA) or semi-local (GGA) type approximations is remarkably similar to Eq. (26). Since LDA and GGA type forms deliver only one exchange–correlation potential and hence only one set of eigenvalues, TDP assumed that these local (loc) forms give rise to an exchange–correlation potential which approximately averages over the difference between the limiting $v_{xc}^{-,\sigma}$ and $v_{xc}^{+,\sigma}$. Using this assumption they arrived at the formula

$$A^\sigma = -(\varepsilon_L^{\mathrm{loc},\sigma} + \varepsilon_H^{\mathrm{loc},\sigma} + I^\sigma) \quad (27)$$

Here we have generalised the original expression to include spin. The term $-(\varepsilon_H^{\mathrm{local},\sigma} + I^\sigma)$ arises as a correction to the conventional Koopmans-type estimate

$$A^\sigma = -\varepsilon_L^{\mathrm{loc},\sigma}. \quad (28)$$

The corresponding Koopmans-type estimate of the ionization potential is

$$I^\sigma = -\varepsilon_H^{\mathrm{loc},\sigma}. \quad (29)$$

The TDP formula corresponds to correcting the orbital in the Koopmans type expression by a downwards shift $\Delta_{xc}^\sigma/2 = (v_{xc}^{+,\sigma} - v_{xc}^{-,\sigma})/2 \approx (\varepsilon_H^{\mathrm{loc},\sigma} + I^\sigma)$ (in the limits a constant over all space, except at $r = \infty$ where it drops sharply to zero[12]), to account for the necessary deficiencies associated with the orbital energies arising from local functionals. We now consider an alternative route to this expression, which will illustrate the importance of the averaging assumption to the utility of the TDP expression.

Let us consider a fictitious exchange–correlation functional which is explicitly density dependent such that at the integer N, $N-1$ and $N+1$ particle systems the exact ground state electronic energy is obtained. Furthermore, let us assume that off integer this functional suffers from MSIE. Since the functional is explicitly density dependent it also delivers only a single uniquely defined Kohn–Sham exchange–correlation potential for each spin, v_{xc}^σ, at both the off integer (in common with the exact functional) and integer systems (specific to local differentiable approximations). We do not assume any averaging behaviour. If the functional gives rise to a convex MSIE between the integers then the E vs. M curve will look like the schematic in Figure 1.

From the graphical representations of Figure 1 it is clear that the errors in the Koopmans estimates of Eq. (28) and Eq. (29) can be calculated as

$$\lambda_+^\sigma = -A^\sigma - \varepsilon_L^{\mathrm{fic},\sigma} \quad (30)$$

$$\lambda_-^\sigma = I^\sigma + \varepsilon_H^{\mathrm{fic},\sigma} \quad (31)$$

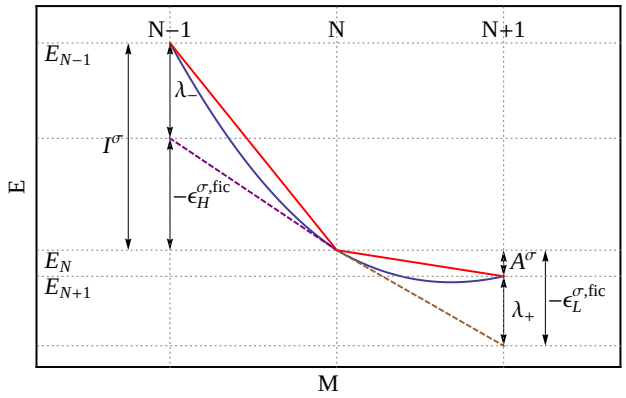

Fig. 1 Schematic of the electronic energy vs. the average particle number, M, for species with $Z-1 \leq M \leq Z+1$, where Z is the atomic number. The red lines correspond to the ensemble energy of Eq. (3), the slopes of which are $\mu^{-,\sigma} = -I^\sigma$ and $\mu^{+,\sigma} = -A^\sigma$ on the deficient and abundant sides of the integer respectively (see Eqs. (6) and (7)). See text for further discussion. The blue lines correspond to the energy computed using the Kohn–Sham self consistent density and orbitals at each average particle number M. The dashed lines are the initial slopes of the energy calculated using the self-consistent Kohn–Sham solutions on the deficient (purple) and abundant (brown) sides of the integer and are consistent with the use of Janak's theorem in Eqs. (23) and (24). Also shown are the ionization potential and electron affinity of the N particle system defined by Eqs. (8) and (9) along with their Koopmans type estimates (HOMO eigenvalues) defined in Eqs. (29) and (28). The quantities $\lambda_\pm$ represent the errors in the Koopmans type estimates of I^σ and A^σ defined in Eqs. (31) and (30), arising from the deviation of the approximate energies from linearity and lack of $\Delta_{\mathrm{xc}}^\sigma$

Note that these expressions are valid for any of the exchange-correlation potentials defined up to an additive constant c. However, unless the potentials on each side of the integer are fixed to approach an asymptotic value of 0 the associated eigenvalues will not be the slopes of the dashed lines shown. Instead they would represent slopes reflecting the shift in v, consistent with an appropriately modified form of Janak's theorem[37] off integer. We note the similarity of the error expression for λ_-^σ to the correction term used by TDP. However, no assumption of averaging has been employed. If we consider the two limiting potentials $v_{\mathrm{xc}}^{-,\sigma}$ and $v_{\mathrm{xc}}^{+,\sigma}$, along with their average $v_{\mathrm{xc}}^{\mathrm{avg},\sigma} = (v_{\mathrm{xc}}^{-,\sigma} + v_{\mathrm{xc}}^{+,\sigma})/2$, then it is clear that if the potential obtained from the fictitious approximation lies in between the abundant and deficient sides then $\varepsilon_H^{\mathrm{fic},\sigma} - \varepsilon_H^{-,\sigma} = \varepsilon_H^{\mathrm{fic},\sigma} + I > 0$, and $\varepsilon_L^{+,\sigma} - \varepsilon_L^{\mathrm{fic},\sigma} = -A^\sigma - \varepsilon_L^{\mathrm{fic},\sigma} > 0$. If the potential of the fictitious functional is shifted below the deficient limiting potential then the first inequality reverses; if it is shifted above the abundant limiting potential then the second inequality is reversed.

The quantity $\lambda_+^\sigma - \lambda_-^\sigma$ is exactly zero when the potential $v_{\mathrm{xc}}^{\mathrm{fic},\sigma} = v_{\mathrm{xc}}^{\mathrm{avg},\sigma}$. This allows us to make the identifications

$$\frac{\Delta_{\mathrm{xc}}^\sigma}{2} = -A^\sigma - \varepsilon_L^{\mathrm{fic},\sigma} = \lambda_+^\sigma \quad \Longleftrightarrow \quad v_{\mathrm{xc}}^{\mathrm{fic},\sigma} = v_{\mathrm{xc}}^{\mathrm{avg},\sigma} \tag{32}$$

$$\frac{\Delta_{\mathrm{xc}}^\sigma}{2} = I^\sigma + \varepsilon_H^{\mathrm{fic},\sigma} = \lambda_-^\sigma \quad \Longleftrightarrow \quad v_{\mathrm{xc}}^{\mathrm{fic},\sigma} = v_{\mathrm{xc}}^{\mathrm{avg},\sigma} \tag{33}$$

where the first equality in each case holds only when the functional potential exactly averages. Using the assumption that this is always the case for (semi-) local density-functional approximations, the expression of TDP is readily derived by equating the two expressions for $\frac{\Delta_{\mathrm{xc}}^\sigma}{2}$.

More generally from this derivation we see that the difference $\lambda_+^\sigma - \lambda_-^\sigma$ measures the extent to which the potential averaging assumption holds. If the potential lies between the deficient and abundant sides then $\lambda_+^\sigma > 0$ and $\lambda_-^\sigma > 0$, if the potential is shifted above the abundant side then $\lambda_+^\sigma < 0$ and $\lambda_-^\sigma > 0$ and if it is shifted below the deficient side then $\lambda_+^\sigma > 0$ and $\lambda_-^\sigma < 0$. Hence by studying the properties of λ_+^σ and λ_-^σ we can determine the extent to which the averaging assumption is holding and hence the reliability of the TDP formula.

2.4 Lowest excited states with symmetries different to the ground state

It is interesting to note that Eq. (27) states that one must always consider the ionization potential of the same spin as the electron being added to the N-electron system to form the anion in order to calculate its electron affinity. This is a consequence of the structure of unrestricted Kohn–Sham theory. In this approach there are two separate discontinuities, one for each spin (see Eq. (16)) and to determine the affinity of a given spin via Eq. (27) it is required to determine the correction due to the discontinuity of the same spin. This means that sometimes the ionization potential must be calculated from the HOMO of a given spin that may not necessarily be the overall HOMO of the atom or molecule. As such, in some cases the relevant ionization process leads to an excited state of the cation rather than its ground state.

In general, density-functional theory is considered a ground state theory. However, it has been shown that some excitation energies may be calculated in a ΔSCF manner by performing calculations on the ground and excited states directly. This approach has been shown to be valid for the lowest excited states having a different symmetry to the ground state[44,45], with the caveat that the exact exchange–correlation functional for the excited states should be symmetry dependent. However, in practice the further approximation is usually made to utilize the same approximate functionals as for the ground states. The states obtained in this manner are rigorously excited states and are orthogonal to the ground state by symmetry, though the quality of the resulting calculations will vary with the type

of excited state considered and the similarity of its electronic structure to the ground state[46–48].

The ground and excited states obtained from the N-electron system via ionization from the HOMOs of different spin belong to different symmetries. We can therefore perform SCF calculations in order to determine their energies at the integers using standard unrestricted Kohn–Sham theory for specific symmetries. The ensemble energies may then be calculated between the integers via Eq (3), where E_0 is then the lowest state of a specified symmetry. The Kohn–Sham equations can also be solved for the excited states at each fractional average particle number M as described in Section 2.1 for the ground state. In Section 3 we will present specific numerical examples where excited states of the cation are utilized in Eq (27).

3 Results and discussion

Throughout this study we consider the elements Li–Cl and Ga–I. For the elements Li–Cl calculations were performed using the aug-cc-pVTZ[49–52] basis set. The noble gas elements are omitted throughout this work since their (negative) electron affinities are unknown experimentally. For Li–Cl, in addition to the calculation of electron affinities via Eqs. (9), (27), and (28) we also present the analysis of E vs. M curves of the type schematically presented in Figure 1. For the heavier elements only the p-block atoms Ga–I are included since comparable basis sets are lacking for K, Ca, Rb and Sr. For the atoms In–I relativistic pseudo-potentials have been employed with the aug-cc-pVTZ-PP basis set[53]. In order to ascertain the accuracy of our basis sets for the calculation of electron affinities, test calculations at the CCSD(T) level were performed for all atoms yielding mean absolute errors of just 0.14 eV for I and 0.15 eV for A. Considering only the atoms In–I, where relativistic pseudo potentials are employed, the mean absolute error rises to 0.25 eV for I and remains at 0.15 eV for A. As a reference throughout this work we use the experimental values from the recent compilation of Ayers *et al.*[54] Preliminary studies also indicated that the pseudo-potential approach was not sufficiently reliable for elements heavier than I. Cartesian basis functions were utilized throughout. The standard PBE calculations in this study were performed with the Gaussian 09[55] program and the PBE calculations for fractional particle numbers were performed with a development version of the Dalton2013[56,57] program.

3.1 Electron affinities and the E vs. M analysis

Table 1 presents electron affinities determined using Eq. (9), Eq. (27) and Eq. (28); also listed are the PBE ionisation potentials and orbital energies (for the neutral N-electron systems) used in the TDP expression. Firstly, consider the DFT affinities determined as an electronic energy difference, Eq. (9). Despite the formal difficulties associated with direct calculations on the anion, the results for all of the atoms in Table 1 are in very good agreement with the experimental values, with a mean absolute error of just 0.18 eV. The accuracy of such estimates using conventional density-functional approximations and basis sets has been discussed widely in the literature[1,3–6,8] and is well understood. In addition to the mean and mean absolute errors d and $|d|$, the linear regression parameters for a correlation plot between the calculated and experimental values, m, c and r^2 are also presented. The high quality of the estimates using the PBE energies in Eq. (9) is clear with m, c and r^2 close to their ideal values of 1, 0 eV and 1, respectively.

Next we consider the electron affinities determined using the Koopmans-type estimate of Eq. (28). From the discussion in Section 2 we do not expect these values to be accurate, except in the extreme case that $\lambda_+ = 0$. In the best-case scenario that the exchange–correlation potential associated with the PBE approximation instead averages over $\Delta_{\rm xc}$ then the values predicted in this manner should be in error by $\Delta_{\rm xc}/2$. The values in Table 1 are consistent with the expected inaccuracy of this expression, exhibiting systematic overestimations of A, with $|d|$ of 3.43 eV. The correlation between the experimental affinities and the Koopmans-type estimates is also poor with m, c and r^2 of 0.56, -1.25 eV and 0.80, respectively.

The TDP expression of Eq. (27) was derived to account explicitly for the lack of a $\Delta_{\rm xc}$ contribution for (semi-) local functionals under the assumption that they average over $\Delta_{\rm xc}$, such that $\lambda_+ \approx \lambda_-$. As discussed in Section 2 the TDP expression may be thought of as a corrected Koopmans-type expression. The results for this expression are presented in column six of Table 1, it is clear from these values that the quality of the results obtained is mixed, with a systematic tendency to underestimate A. In particular, large errors are evident for the atoms Li and Na. In Figure 2 the deviations from the experimental values are presented for each atom. The breakdown for the Li and Na atoms is clearly evident. In addition it is clear that in general as the atomic number increases the errors in the TDP predictions of the electron affinities decrease. The largest errors observed are for the s-block elements Li, Be, Na and Mg. It is also evident that for the heavier p-block elements the Group 15 elements P, As and Sb display larger errors than the other p-block elements from the same rows of the periodic table.

The breakdown for Li and Na may have been anticipated because the electron addition and subtraction processes involve different principal quantum numbers: For Li, the electron is added to 2s orbital but removed from the 1s, whilst for Na, the electron is added to 3s orbital but removed from 2p. This would lead us to expect the problem to be more pronounced for Li, as is indeed observed in Figure 2. Based on similar

Table 1 PBE HOMO and LUMO energies $\varepsilon^{\sigma}_{\mathrm{HOMO}}$ and $\varepsilon^{\sigma}_{\mathrm{LUMO}}$, ionization energies I and electron affinity estimates using Eq. (9), (27) and (28), together with the reference experimental electron affinities. In the case of group III and group IV elements, $\sigma = \alpha$, whereas for the group VI and VII elements, $\sigma = \beta$. The error measures are presented over the p-block elements only. d and $|d|$ denote mean and mean absolute errors, respectively, relative to the experimental values. m, c, and r^2 denote the gradient, intercept, and correlation parameters, respectively, of the correlation curves, relative to the experimental values. All affinity estimates, errors and intercepts are given in eV; all other quantities are in a.u.

Atom	I	$\varepsilon^{\sigma}_{\mathrm{HOMO}}$	$\varepsilon^{\sigma}_{\mathrm{LUMO}}$	Eqn. (9)	Eqn. (27)	Eqn. (28)	$A_{\mathrm{Exp.}}$
Li	2.353	-0.169	-0.006	0.51	-59.27	0.16	0.62
Be	0.331	-0.206	-0.074	-0.02	-1.38	2.01	0.30
B	0.318	-0.153	-0.133	0.61	-0.88	3.62	0.28
C	0.424	-0.224	-0.205	1.58	0.14	5.58	1.26
N	0.755	-0.562	-0.152	0.27	-1.11	4.13	-0.18
O	0.517	-0.279	-0.239	1.77	0.02	6.49	1.46
F	0.649	-0.378	-0.342	3.66	1.95	9.31	3.40
Na	1.428	-1.057	-0.052	0.55	-8.66	1.42	0.55
Mg	0.280	-0.173	-0.049	-0.05	-1.57	1.34	0.54
Al	0.223	-0.114	-0.102	0.58	-0.20	2.77	0.43
Si	0.301	-0.169	-0.161	1.49	0.78	4.37	1.39
P	0.594	-0.441	-0.137	0.88	-0.43	3.74	0.75
S	0.383	-0.226	-0.207	2.17	1.36	5.63	2.08
Cl	0.477	-0.299	-0.284	3.65	2.89	7.73	3.61
Ga	0.220	-0.109	-0.100	0.48	-0.31	2.71	0.43
Ge	0.291	-0.162	-0.157	1.44	0.77	4.27	1.23
As	0.613	-0.458	-0.134	0.89	-0.56	3.65	0.81
Se	0.355	-0.211	-0.199	2.13	1.49	5.41	2.02
Br	0.434	-0.274	-0.266	3.49	2.90	7.25	3.36
In	0.205	-0.104	-0.097	0.53	-0.13	2.63	0.38
Sn	0.267	-0.151	-0.148	1.42	0.89	4.04	1.11
Sb	0.571	-0.428	-0.129	0.95	-0.36	3.52	1.05
Te	0.321	-0.193	-0.185	2.07	1.58	5.04	1.97
I	0.386	-0.247	-0.242	3.25	2.80	6.59	3.06
d				0.17	−0.82	3.43	
$\|d\|$				0.18	0.82	3.43	
m				1.01	0.84	0.56	
c				−0.19	0.92	−1.25	
r^2				0.99	0.90	0.80	

arguments, we can also rationalize the errors observed for Be and Mg, since the addition and subtraction involves orbitals with different l quantum numbers, that the errors here are less severe reflects the fact that the changes occur between orbitals in shells that share the same principal quantum number.

For the Group 15 elements N, P, As, and Sb the subtraction process involves the removal of an unpaired α-electron, whilst the addition process involves the pairing of electrons. This observation rationalizes the slightly larger errors observed for the elements P, As and Sb in Figure 2. The N atom results are more accurate than these arguments would suggest, however, we note that this is the only atom for which the experimental electron affinity is negative and this may explain its anomalous behaviour. For all the other atoms, the addition and subtraction occurs for electrons of the same spin within a single manifold of p-orbitals, and so the assumption of symmetry is most valid.

A summary of the errors associated with the electron affinity expressions of Eqs. (9), (27) and (28) is given by the normal

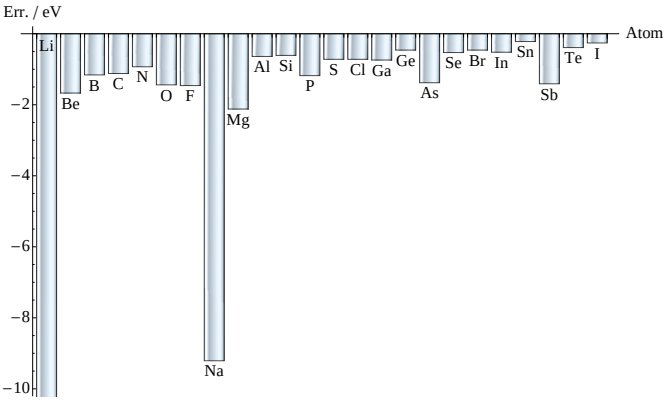

Fig. 2 Errors in eV for the atomic electron affinities predicted by Eq. (27) relative to experimental values. Large errors are predicted for cases where the assumptions underlying the TDP expression are expected to break down e.g. for Li and Na. For the heavier p-block elements the errors for the Group 15 elements P, As and Sb elements are slightly larger than the other p-block elements in the same rows of the periodic table, see text for further discussion. Note that the bar for Li is truncated and corresponds to an error of −59.88 eV

distributions in Figure 3 for the p-block atoms only. The positions of the centres of the distributions relative to the ordinate reflect the quality of the mean errors, whilst the width of the distributions reflect the standard deviations of the errors associated with each expression relative to the experimental values in Table 1. The quality of the conventional affinity estimates associated with Eq. (9) is clearly reflected by the width and position of the blue peak. The large spread of errors and the systematic overestimation of A by the Koopmans-type expression of Eq. (28) is reflected by the brown peak. Finally the red peak represents the substantial improvement the TDP expression of Eq. (27) offers over the Koopmans-type estimates for the p-block atoms.

As was discussed in Section 2 the quality of the averaging assumption underlying the TDP expression for the electron affinity may be quantified by the difference between the quantities λ_- and λ_+, which may be related to a plot of E vs. M. To further understand the trends in the errors presented in Figure 2 and Table 1 the E vs M curves for the elements Li–F with $Z-1 \leq M \leq Z+1$ are presented in Figures 4 and 5. The ensemble energies calculated using the ground state PBE energies are shown as red lines and have slopes on either side of the integer particle number $M = Z$ that are equal to the PBE estimates of the ionization potential and electron affinity according to Eqs. (8) and (9). The variational PBE energies calculated at non-integer particle number M are shown as blue lines, the initial slopes of the variational PBE energies on either side of the integer are shown as dashed lines and have been calculated by forward and backward finite difference with a spacing of 0.001 in M. The numerical initial

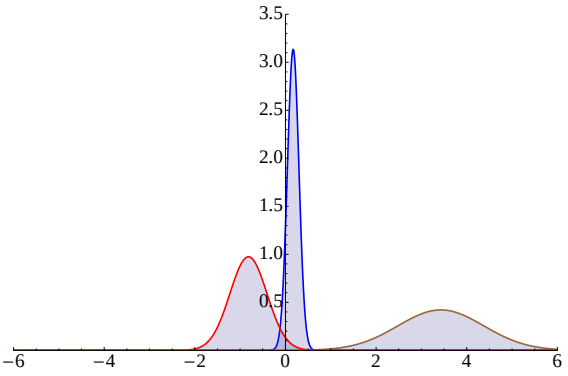

Fig. 3 Normal distributions of errors in PBE electron affinities (in eV) of the p-block elements, relative to experimental values, calculated using the ΔSCF formula of Eq. (9) (blue), the corrected Koopmans formula of Eq. (27) (red) and the standard Koopmans formula of Eq. (28) (brown).

slopes s_- and s_+ are equal to the PBE orbital energies, $\varepsilon_H^{\rm PBE}$ and $\varepsilon_L^{\rm PBE}$ respectively, at the integer particle number $M = Z$ consistent with Eqs. (29) and (28) and $\Delta_{\rm xc}^{\rm PBE} = 0$. The PBE estimates of λ_+ and λ_- are also indicated in each plot, along with the difference $\lambda_+ - \lambda_-$. The key quantities in understanding the quality of the PBE TDP estimates of A^σ are then the discrepancies between the ensemble and variational PBE initial slopes, which are quantified by λ_- and λ_+.

For the atoms Li–F the E vs. M plots are presented in Figure 4. For the Li atom the large discrepancy between the λ_- and λ_+ values is clear, with λ_- being large and positive whilst λ_+ is small and close to zero. This indicates that the averaging assumption is very poor, consistent with the breakdown of the TDP expression for this atom as shown in Table 1. In addition since $\lambda_+ \approx 0$ the Koopmans-type expression of Eq. (28) is expected to be uncharacteristically accurate. This is indeed borne out by the values in Table 1 with an error of just 0.46 eV, compared to the TDP error of −59.89 eV. This error however is still not competitive with the conventional estimate using Eq. (9), which has an error of 0.11 eV. For the remaining first row atoms the averaging assumption appears to be much more well founded with values of $\lambda_+ - \lambda_-$ between 0.050 and 0.065 $E_{\rm h}$. The size of these errors and their relative consistency reflects the nature of the errors over the p-block elements presented in Figures 2 and 3.

The E vs. M curves for Na–Cl are presented in Figure 5. In general the errors in the TDP estimates of the electron affinities decrease as Z increases, as shown in Figure 2. This trend is reflected in the $\lambda_+ - \lambda_-$ values presented in Figure 5 when compared with those in Figure 4. The value of $\lambda_+ - \lambda_-$ for Na atom is large, consistent with that for Li and reflecting the large errors in the TDP prediction due to a breakdown of the averaging assumption. The values of $\lambda_+ - \lambda_-$ for the second row p-block elements are substantially reduced compared to the first row p-block elements, consistent with the trend in Figure 2. It is notable that the reduction in $\lambda_+ - \lambda_-$ as Z increases is substantially less for the Group 15 elements than for other members of the p-block. This trend is also evident in Figure 2 for the heavier elements of the p-block.

The noble gas atoms have been omitted from our analysis since their electron affinities are unknown. At first sight, the TDP expression would appear to provide a simple route for estimating the negative electron affinities of the noble gas atoms. However, such cases would again involve addition / subtraction to / from orbitals of different principal quantum number (as in Li, Na) and so we anticipate that the resulting affinities would be largely underestimated and hence unreliable.

3.2 Excited state cationic species and the E vs. M analysis

For Li, Na and the Group 15 elements the ionisation process appropriate for the TDP evaluation yields a cation in an excited state, as discussed in Section 2. For all the other atoms, the ground state cation is obtained. To our knowledge the E vs. M analysis presented here and elsewhere in the literature [11,16–24] has only been applied to the ground states of atomic and molecular systems. In Figures 4 and 5 we have presented plots in which the ionization of these species leads to excited states of the cation (albeit the lowest state of a given symmetry), as required by Eq. (27) and discussed in Section 2. That such a situation arises is a consequence of the structure of unrestricted Kohn–Sham spin-DFT, the context in which we apply ZTGC-EDFT.

To illustrate the significance of choosing to ionize an electron from the HOMO of the same spin as the LUMO into which an electron is added we consider the phosphorus atom in detail. In Figure 6 we present three possible E vs. M curves corresponding to the following situations: (i) the cationic system is in an excited state, the neutral and anionic systems in their ground states, (ii) the cationic, neutral and anionic systems are all in their ground states and (iii) the cationic and neutral systems are in the ground state, the anionic system is in an excited state. Case (i) corresponds to ionization from the β-HOMO of the neutral system and electron addition to the β-LUMO and is of relevance to determine the discontinuity $\Delta_{\rm xc}^\beta$ and hence the ground state estimate of A^β via the TDP expression. The red lines in case (ii) have slopes corresponding to the ground state ionization potential and electron affinity, the discontinuity between the slopes of these lines is of relevance to determining the ground state molecular hardness or fundamental band gap, this connection will be explored in more detail in Section 3.3. Case (iii) corresponds to electron removal from the α-HOMO and electron addition to the α-LUMO and so is of relevance to determining the discontinuity $\Delta_{\rm xc}^\alpha$. It is notable that the quantity $\lambda_+ - \lambda_-$ is much smaller for case (i)

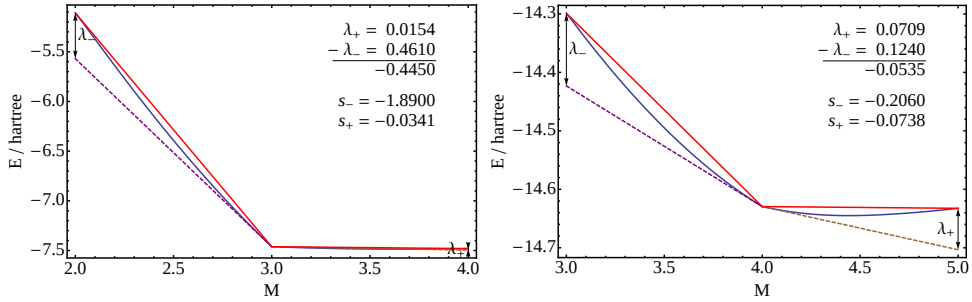

(a) Z=3

(b) Z=4

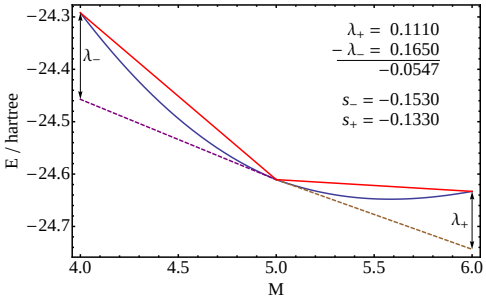

(c) Z=5

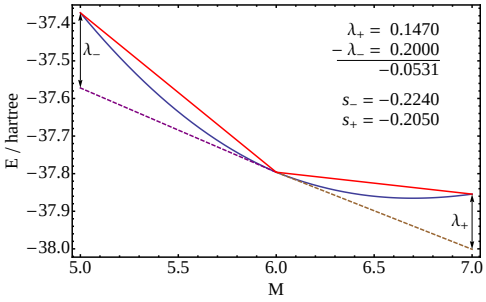

(d) Z=6

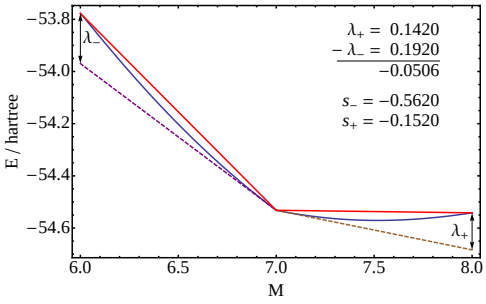

(e) Z=7

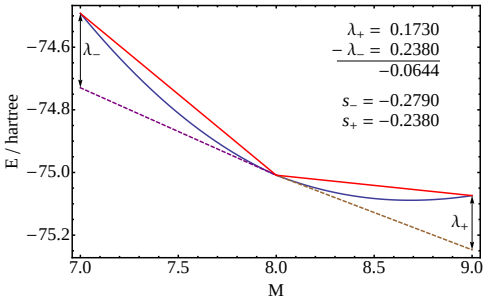

(f) Z=8

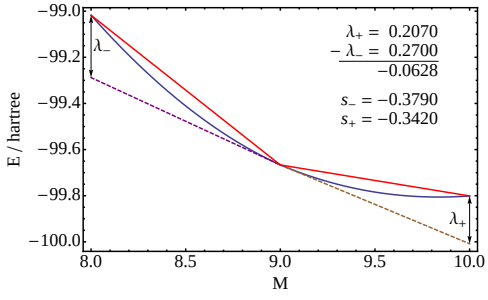

(g) Z=9

Fig. 4 E vs. M curves calculated using the PBE functional using the aug-cc-pVTZ basis set for the atoms Li–F with $Z-1 \leq M \leq Z+1$

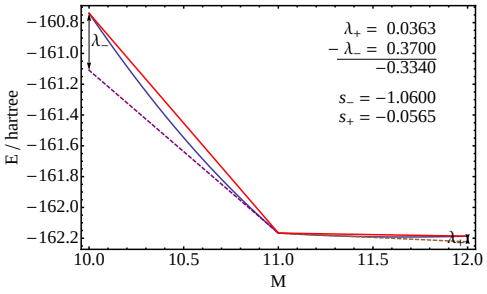

(a) Z=11

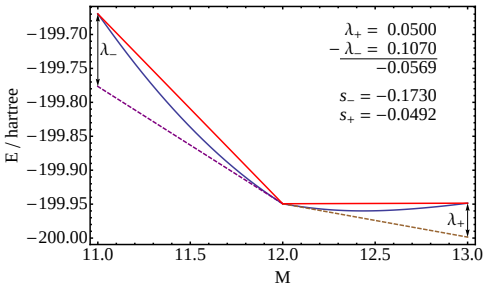

(b) Z=12

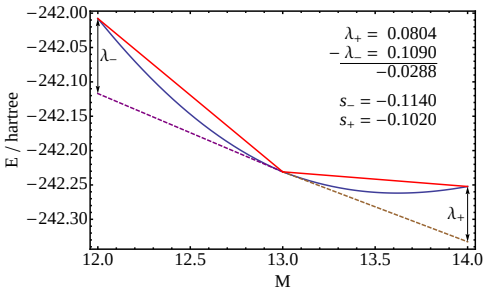

(c) Z=13

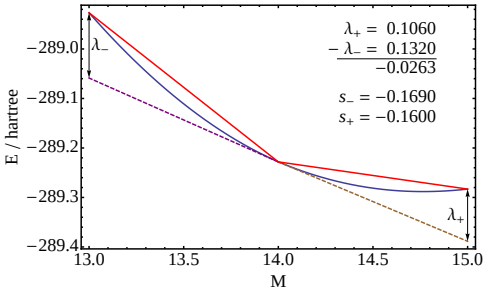

(d) Z=14

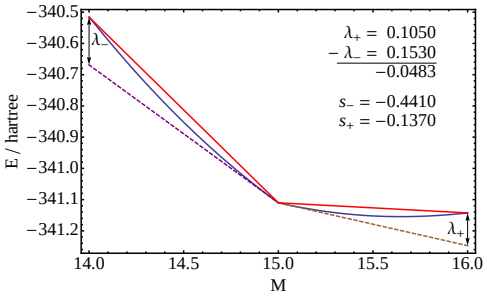

(e) Z=15

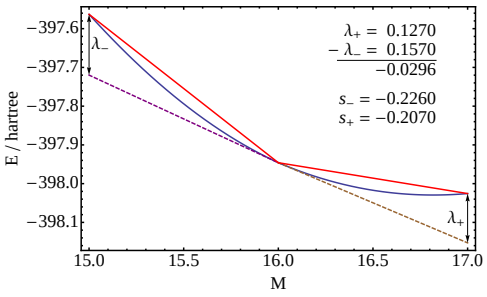

(f) Z=16

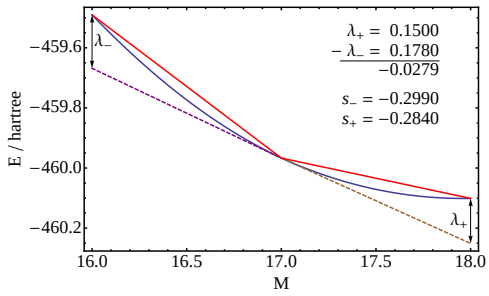

(g) Z=17

Fig. 5 E vs. M curves calculated using the PBE functional using the aug-cc-pVTZ basis set for the atoms Na–Cl with $Z-1 \leq M \leq Z+1$

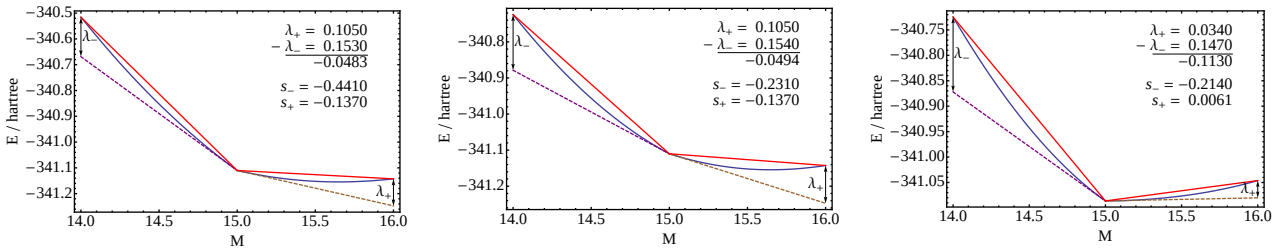

Fig. 6 E vs. M plots for the phosphorus atom. In the left the panel the cation is in an excited state with multiplicity 5, corresponding to ionization from the β-HOMO of the neutral system, the anion is in its ground state corresponding to electron addition to the β-LUMO. In the central panel, the cation is in its ground state configuration with multiplicity 3, corresponding to ionization from the α-HOMO, the anion is also in its ground state configuration corresponding to electron addition to the β-LUMO. In the right panel the cation is in its ground state corresponding to ionization from the α-HOMO, whilst the anion is in its excited state corresponding to electron addition to the α-LUMO. See text for further discussion

than case (iii). This in turn implies that the $v_{\rm xc}^{{\rm PBE},\beta}$ potential is closer to averaging over the $\Delta_{\rm xc}^{{\rm PBE},\beta}$ discontinuity than $v_{\rm xc}^{{\rm PBE},\alpha}$ is to averaging over the $\Delta_{\rm xc}^{{\rm PBE},\alpha}$ discontinuity.

In Figure 7 the potentials $v_{\rm xc}^{{\rm PBE},\alpha}$ and $v_{\rm xc}^{{\rm PBE},\beta}$ are presented along with the corresponding potentials on the electron deficient and electron abundant sides of the integer. Consistent with the analysis in terms of $\lambda_+ - \lambda_-$ values presented here, the α PBE potential is closer to the PBE potential corresponding to the abundant side of the discontinuity than the deficient side of the integer. The β PBE potential on the other hand is closer to averaging over the potentials on the deficient and abundant sides of the integer, consistent with the reasonable accuracy of the TDP expression and the $\lambda_+ - \lambda_-$ values in Figure 6.

3.3 Mulliken electronegativity and absolute hardness

We now use the analysis presented in the previous sections to compute two global reactivity indices introduced in conceptual DFT. [58–67]. Within this framework, global and local reactivity indices are introduced as response functions of the energy of the system with respect to the number of electrons and/or the external potential.

Two important global quantities that will be studied here are the electronegativity[68,69], according to the Mulliken definition[70], and the absolute chemical hardness, introduced by Parr and Pearson[71]. The former quantity is given by

$$\chi_{\rm M} = \frac{I_0 + A_0}{2} \tag{34}$$

where the ground state ionization potential I_0 and electron affinity A_0 are used. As was discussed in Section 2 and emphasized in the analysis of the P atom in Section 3.1 the determination of ground state properties relates to the ground state E vs. M curves. The (absolute) chemical hardness is given by

$$\eta = \frac{I_0 - A_0}{2} \tag{35}$$

The concept of chemical hardness was introduced qualitatively in the late 1950s and early 1960s by Pearson in the framework of his classification of Lewis acids and bases[72–74]. This quantity also measures the size of the discontinuity between the slope of the E vs. M plots on either side of the integer $M = Z$ and is related to the ground state fundamental gap of Eq. (17) by a factor of two. This working formula arises from a three point finite difference approximation using the energies at the integer particle numbers $M = Z-1$, $M = Z$ and $M = Z+1$. This is consistent with a quadratic fit to the three points and selects a derivative at the integer which is equal to the average of the left and right derivatives of the ground state E vs. M plots at $M = Z$.

The values of η and $\chi_{\rm M}$ in Eqs. (35) and (34) can be evaluated using either computed or experimental ionization energies and electron affinities. The quantities determined using the experimental values are here used as a reference, against which we measure the reliability of the computed quantities. We will compute both quantities via three routes, based on the arguments presented in Section 2.

The first approach uses Eqs. (34) and (35) but with I_0 and A_0 computed from PBE ΔSCF values; this will be referred to as the conventional evaluation. For the second approach, we first rewrite Eqs. (34) and (35) in terms of the Kohn-Sham orbital energies following Eq. (31) and (30); note that, from now on, we have dropped the label "fic." in the equations. It is important to note that the latter equations are dependent on the spin label and that Eqs. (34) and (35) necessarily always use the ground state I_0 and A_0. In the following expressions, we will thus write in general that $I^0 = I^{\sigma'}$ and $A^0 = A^{\sigma}$.

$$\chi_{\rm M} = \frac{I^{\sigma'} + A^{\sigma}}{2} = -\frac{\varepsilon_H^{\sigma'} + \varepsilon_L^{\sigma}}{2} - \frac{(\lambda_+^{\sigma} - \lambda_-^{\sigma'})}{2} \tag{36}$$

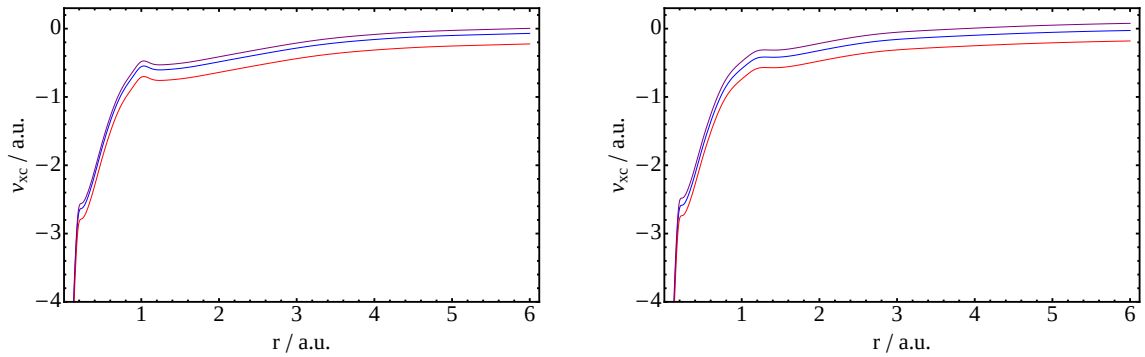

Fig. 7 The PBE exchange-correlation potentials for the P atom. In the left-hand panel the α-spin potentials $v_{xc}^{\alpha,+}$ (purple), $v_{xc}^{\alpha,-}$ (red) and v_{xc}^{α} (blue) are presented. The potentials on the abundant and deficient sides are determined using the PBE Δ-SCF estimates of I and A. In the right-hand panel the analogous β-spin potentials $v_{xc}^{\beta,+}$ (purple), $v_{xc}^{\beta,-}$ (red) and v_{xc}^{β} (blue) are presented. See text for discussion

and

$$\eta = \frac{I^{\sigma'} - A^{\sigma}}{2} = \frac{\varepsilon_L^{\sigma} - \varepsilon_H^{\sigma'}}{2} + \frac{(\lambda_+^{\sigma} + \lambda_-^{\sigma'})}{2} \tag{37}$$

Introducing the TDP approximation for λ_+^{σ} and keeping $I^{\sigma'}$, these equations can be rewritten as

$$\chi_{\mathrm{M}} = \frac{I^{\sigma'} + (-\varepsilon_H^{\sigma} - \varepsilon_L^{\sigma} - I^{\sigma})}{2} \tag{38}$$

and

$$\eta = \frac{I^{\sigma'} - (-\varepsilon_H^{\sigma} - \varepsilon_L^{\sigma} - I^{\sigma})}{2} \tag{39}$$

These equations, Eqs. (38) and (39), will be referred to as the TDP expressions for χ_{M} and η, respectively and will be evaluated using the PBE ΔSCF estimates of $I^{\sigma'}$ and I^{σ}.

In line with the previous discussion of electron affinities we also consider a third pair of expressions which we will refer to as the Koopmans-type estimates of the same quantities. These expressions are obtained by replacing the ionization potential and electronic affinity in Eqs. (34) and (35) by the negative of the HOMO and LUMO eigenvalues giving

$$\chi_{\mathrm{M}} \approx -\frac{\varepsilon_L^{\sigma} + \varepsilon_H^{\sigma'}}{2} \tag{40}$$

$$\eta \approx \frac{\varepsilon_L^{\sigma} - \varepsilon_H^{\sigma'}}{2} \tag{41}$$

Table 2 presents the results obtained from the conventional, TDP and Koopmans-type evaluations of χ_{M} and η. The PBE estimates of χ_{M} obtained via Eq. (34) are very close to the estimates based on experimental values of I_0 and A_0, reflecting the accuracy of the conventional PBE estimates of these quantities. The mean and mean absolute errors are just 0.12 and 0.14 eV respectively. Comparing the estimates obtained using the TDP expression of Eq. (38) with those from the Koopmans-type expression of Eq. (40) as presented in columns three and four of Table 2, it is clear that only the estimates for Li, N, Na, P, As, and Sb differ between the two due to the cancellation of the integer discontinuity correction terms in the TDP expression when the processes of electron addition and subtraction involve electrons of the same spin (see Eq. (36)).

This cancellation means that in general the Koopmans estimate of the electronegativity may be reasonably reliable, as quantified by the mean and mean absolute errors of −0.38 eV and 0.38 eV relative to the values derived from experiment over the p-block atoms. For Li and Na large discrepancies are observed between the TDP and experimental results. These may be understood as arising due to the breakdown of the assumption that $\lambda_+ \approx \lambda_-$ as discussed in the last section.

For the group 15 elements N, P, As and Sb the differences between the TDP and Koopmans results show mixed performance; for N the TDP value is substantially closer to the experimental value than the Koopmans value, for P the values are comparable and for As and Sb the TDP values underestimate the experimental values by more than the Koopmans estimates. The quality of the results for each approach is summarized for the p-block elements (where the averaging assumption holds reasonably well) in Figure 8. The blue distribution reflects the reasonable quality of the PBE estimates. The brown distribution shows the systematic underestimation of the electronegativity using the Koopmans approximation, although it is more accurate than may otherwise be expected due to the cancellation of the integer discontinuity terms for all but N, P, As and Sb. The TDP expression which accounts for these corrections leads to little improvement in the quality of the results, though the width of the distribution is narrowed reflecting a slightly reduced spread in the errors relative to experiment.

For the chemical hardness, η, the conventional estimates

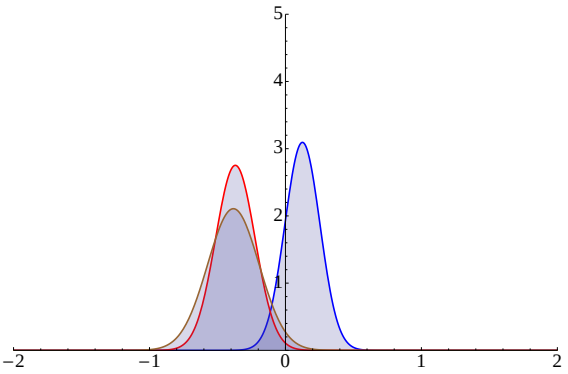

Fig. 8 Normal distributions for the errors (in eV) in the Mulliken electronegativities χ_M relative to experiment calculated using Eq (34) (blue), Eq. (38) (red) and Eq (40) brown.

using PBE energies again show good accuracy with mean and mean absolute errors relative to the experimental values for the p-block elements of just -0.05 and 0.08 eV, respectively. The Koopmans-type estimates in this case are in substantial error with mean and mean absolute errors of -3.81 and 3.81 eV. The disparity between the quality of the Koopmans-type estimates for χ_M and η may be understood by noting that in the derivation of the TDP expressions for these quantities the integer discontinuity corrections cancel for χ_M but not for η, as can be seen from Eq. (36) and (37) . The impact of this is clearly evident in column six of Table 2. Again the values for Li and Na are in substantial error due to the break down of the assumption that $\lambda_+ \approx \lambda_-$, however, for the other species the TDP estimates are much closer to the experimental values. This is reflected in the errors over the p-block elements with mean and mean absolute errors both of 0.45 eV representing a substantial improvement over the Koopmans-type estimates. Figure 9 summarizes the quality of the results. The high quality of the conventional estimates is clearly shown by the blue distribution which is sharply peaked and close to the ordinate. The poor quality of the Koopmans-type estimates is clear, the brown distribution being very broad and showing systematic underestimation of the estimates of η for the p-block elements. The red distribution emphasizes the clear improvement obtained for the TDP estimates, giving a much an narrower distribution closer to the ordinate with a slight tendency to overestimate η.

4 Conclusion

The natural framework for treating systems with fractional particle number in the context of density-functional theory is ZTGC-EDFT. In this work we have given a short overview of the aspects of this theory relevant to determining the electron affinity, electronegativity and chemical hardness of a range of atomic species in the context of spin-DFT. The essential aspects of our analysis are expected to carry over to molecular systems.

Three routes to calculate electron affinities were considered: the conventional ΔSCF approach, the Koopmans-type estimate and a corrected Koopmans-type estimate, designed to account for the exchange–correlation discontinuity, Δ_{xc}, under the assumption that the errors associated with (semi-) local functionals are symmetric with respect to the processes of electron addition / subtraction. This assumption has been quantified in terms of the quantities λ_+ and λ_-, which measure the discrepancy between the (formally but not practically equivalent) ensemble and variational results obtained using approximate (semi-) local density functionals.

In the case that $\lambda_+ \approx \lambda_-$ the TDP (corrected Koopmans) results were found to yield a substantial improvement over Koopmans-type estimates. Failures of the TDP approximation relative to the experimental values were most pronounced for Li and Na and are inline with chemical intuition, from which a breakdown of the symmetry assumption would be expected for these species. In general the accuracy of the TDP expression is not competitive with conventional ΔSCF estimates, however, it does offer the possibility to determine esti-

Table 2 Mulliken electronegativity χ_M and molecular hardness η calculated using the Eqs. (34), (38), (40) and (35), (39), (41), respectively. The error measures are presented over the p-block elements only. d and $|d|$ denote mean and mean absolute errors, respectively, relative to the experimental values. m, c, and r^2 denote the gradient, intercept, and correlation parameters, respectively, for correlation plots relative to the experimental values. All values are given in eV

Atom	Eq. (34)	Eq. (38)	Eq. (40)	Exp. χ_M	Eq. (35)	Eq. (39)	Eq. (41)	Exp. η
Li	3.05	−26.84	1.69	3.00	2.54	32.43	1.53	2.39
Be	4.49	3.81	3.81	4.81	4.51	5.19	1.80	4.51
B	4.64	3.89	3.89	4.29	4.03	4.77	0.27	4.01
C	6.56	5.84	5.84	6.26	4.98	5.70	0.26	5.00
N	7.50	6.81	6.21	7.18	7.23	7.92	2.08	7.36
O	7.92	7.04	7.04	7.54	6.14	7.02	0.55	6.08
F	10.66	9.80	9.80	10.41	7.00	7.86	0.50	7.01
Na	2.95	−1.65	2.23	2.84	2.41	7.01	0.81	2.30
Mg	3.78	3.02	3.02	4.09	3.83	4.59	1.68	3.55
Al	3.33	2.93	2.93	3.21	2.74	3.14	0.16	2.78
Si	4.85	4.49	4.49	4.77	3.35	3.71	0.12	3.38
P	5.69	5.03	5.01	5.62	4.80	5.46	1.28	4.87
S	6.29	5.89	5.89	6.22	4.13	4.53	0.26	4.14
Cl	8.31	7.93	7.93	8.29	4.66	5.04	0.20	4.68
Ga	3.23	2.84	2.84	3.21	2.76	3.15	0.13	2.78
Ge	4.68	4.34	4.34	4.57	3.24	3.57	0.07	3.33
As	5.40	4.67	4.80	5.30	4.51	5.23	1.15	4.49
Se	5.90	5.58	5.58	5.89	3.77	4.09	0.16	3.87
Br	7.65	7.36	7.36	7.59	4.16	4.46	0.11	4.23
In	3.06	2.73	2.73	3.09	2.53	2.86	0.09	2.70
Sn	4.34	4.08	4.08	4.23	2.92	3.19	0.04	3.12
Sb	4.96	4.30	4.49	4.83	4.01	4.66	0.97	3.78
Te	5.39	5.15	5.15	5.49	3.33	3.57	0.11	3.52
I	6.87	6.65	6.65	6.75	3.63	3.85	0.06	3.70
d	0.12	−0.37	−0.38		−0.05	0.45	−3.81	
$\|d\|$	0.14	0.37	0.38		0.08	0.45	3.81	
m	0.97	1.01	1.03		0.98	0.86	1.60	
c	0.03	0.29	0.23		0.12	0.19	3.56	
r^2	1.00	0.99	0.99		1.00	0.98	0.43	

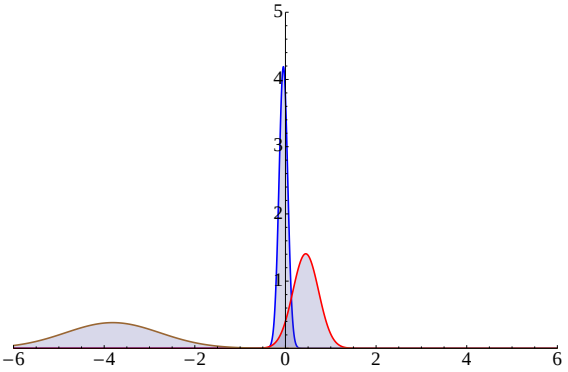

Fig. 9 Normal distributions of the errors (in eV) in the molecular hardness, η, relative to experiment calculated using Eq. (35) (blue), Eq. (39) (red) and Eq. (41) (brown).

mates of A^σ at low cost using (semi-) local functionals without performing troublesome calculations on anionic species.

Central to the interpretation of the quality of the results for each approach was the analysis of E vs. M curves. These plots, whose significance has been evident since the pioneering work of Perdew *et al.*[11], highlight the inconsistency between the ensemble interpolation and variational solutions obtained for local density functional approximations. The initial slopes of the E vs. M curves either side of $M = Z$ are consistent with Janak's theorem and linear extrapolations to $M = Z \pm 1$ were used to define the quantities $\lambda_\pm$. For the Group 15 elements the significance of excited state cation / anion plots for the determination of the spin discontinuities Δ^σ were highlighted. These differ from the more intuitive ground state plots relevant to ground state properties such as the fundamental gap Δ_0.

Finally, we extended the analysis to expressions for the ground state Mulliken electronegativity and the absolute hardness. The working equations for each of these quantities involve the ground state ionization potentials and electron affinities. For the electronegativity the corrections due to the integer discontinuity approximately cancel out and as a consequence the Koopmans and corrected Koopmans expressions yield similar accuracy. For the hardness no such cancellation occurs and the accuracies reflect those obtained for the corresponding electron affinities.

In summary, the TDP expressions represent a computationally inexpensive approach to determine the electron affinity, Mulliken electronegativity and absolute hardness in cases where the errors upon electron addition and subtraction are symmetric, whilst avoiding difficult calculations on anionic species. The TDP expressions are reasonably accurate when the electron addition and subtraction occur within a single manifold of orbitals but fail when these processes involve orbitals with different principal quantum number. To make further progress in this area it may be desirable to seek estimates of the asymmetry quantified in the present work by $\lambda_+ + \lambda_-$.

Acknowledgments

FDP and PG wish to acknowledge the Free University of Brussels (VUB) and the Research Foundation Flanders (FWO) and the for continuous support. A.M.T. is grateful for support from the Royal Society, the Norwegian Research Council through the CoE Centre for Theoretical and Computational Chemistry (CTCC) Grant No. 179568/V30 and the European Research Council under the European Union's Seventh Framework Program through the Advanced Grant ABACUS, ERC Grant Agreement No. 267683. We are grateful to Dr. Espen Sagvolden for helpful discussions.

References

1 H. B. Shore, J. H. Rose and E. Zaremba, *Phys. Rev. B*, 1977, **15**, 2858.
2 K. D. Sen, *Chem. Phys. Lett.*, 1980, **74**, 201.
3 J. M. Galbraith and H. F. Schaefer III, *J Chem. Phys.*, 1996, **105**, 862.
4 N. Rösch and S. B. Trickey, *J Chem. Phys.*, 1997, **106**, 8940.
5 A. A. Jarecki and E. R. Davidson, *Chem. Phys. Lett.*, 1999, **300**, 44.
6 M. Weimer, F. Della Sala and A. Görling, *Chem. Phys. Lett.*, 2003, **372**, 538.
7 F. Jensen, *J. Chem. Theor. Comput.*, 2010, **6**, 2726.
8 D. Lee, F. Furche and K. Burke, *J Phys. Chem. Lett.*, 2010, **1**, 2124.
9 M. C. Kim, E. Sim and K. Burke, *J. Chem. Phys.*, 2011, **134**, 171103.
10 N. D. Mermin, *Phys. Rev.*, 1965, **137**, A1441.
11 J. P. Perdew, R. G. Parr, M. Levy and J. L. Balduz Jr., *Phys. Rev. Lett.*, 1982, **49**, 1691.
12 J. P. Perdew and M. Levy, *Phys. Rev. Lett.*, 1983, **51**, 1884.
13 L. J. Sham and M. Schlüter, *Phys. Rev. Lett.*, 1983, **51**, 1888.
14 E. Sagvolden and J. P. Perdew, *Phys. Rev. A*, 2008, **77**, 012517.
15 F. E. Zahariev and Y. Wang, *Phys. Rev. A*, 2004, **70**, 042503.
16 P. Mori-Sánchez, A. J. Cohen and W. Yang, *J. Chem. Phys.*, 2006, **125**, 201102.
17 A. Ruzsinszky, J. P. Perdew, G. I. Csonka, O. A. Vydrov and G. E. Scuseria, *J. Chem. Phys.*, 2006, **125**, 194112.
18 A. Ruzsinszky, J. P. Perdew, G. I. Csonka, O. A. Vydrov and G. E. Scuseria, *J. Chem. Phys.*, 2007, **126**, 104102.

19 O. A. Vydrov, G. E. Scuseria and J. P. Perdew, *J. Chem. Phys.*, 2007, **126**, 154109.
20 A. J. Cohen, P. Mori-Sánchez and W. Yang, *Phys. Rev. B*, 2008, **77**, 115123.
21 A. J. Cohen, P. Mori-Sánchez and W. T. Yang, *Science*, 2008, **321**, 792.
22 A. J. Cohen, P. Mori-Sánchez and W. T. Yang, *J. Chem. Phys.*, 2008, **129**, 121104.
23 A. J. Cohen, P. Mori-Sánchez and W. T. Yang, *J Chem. Theory Comput.*, 2009, **5**, 786.
24 A. J. Cohen, P. Mori-Sánchez and W. T. Yang, *Chem. Rev.*, 2012, **112**, 289.
25 D. J. Tozer and F. De Proft, *J. Chem. Phys.*, 2007, **127**, 034108.
26 A. J. Cohen, P. Mori-Sánchez and W. Yang, *J. Chem. Phys.*, 2007, **126**, 191109.
27 U. Salzner and R. Baer, *J Chem. Phys.*, 2009, **131**, 231101.
28 T. Stein, H. Eisenberg, L. Kronik and R. Baer, *Phys. Rev. Lett.*, 2010, **105**, 266802.
29 X. Zheng, A. J. Cohen, P. Mori-Sánchez, X. Hu and W. Yang, *Phys. Rev. Lett.*, 2011, **107**, 026403.
30 L. Kronik, T. Stein, S. Refaely-Abramson and R. Baer, *J. Chem. Theory Comput.*, 2012, **8**, 1515.
31 A. Savin, *Recent Developments and Applications of Modern Density Functional Theory*, Elsevier, Amsterdam, 1996, p. 327.
32 D. J. Tozer and F. De Proft, *J. Phys. Chem. A*, 2005, **109**, 8923.
33 F. De Proft, N. Sablon, D. J. Tozer and P. Geerlings, *Faraday Discuss.*, 2007, **135**, 151.
34 A. M. Ejsing and S. B. Nielsen, *J. Chem. Phys.*, 2007, **126**, 154313.
35 S. B. Nielsen and A. M. Ejsing, *Chem. Phys. Lett.*, 2007, **441**, 213.
36 A. M. Teale, F. De Proft and D. J. Tozer, *J. Chem. Phys.*, 2008, **129**, 044110.
37 J. F. Janak, *Phys. Rev. B*, 1978, **18**, 7165.
38 G. K.-L. Chan, *J. Chem. Phys.*, 1999, **110**, 4710.
39 J. Katriel, R. G. Parr and M. R. Nyden, *J. Chem. Phys.*, 1981, **74**, 2397.
40 E. H. Lieb, *Int. J. Quant. Chem.*, 1983, **24**, 243.
41 A. Cedillo, *Int. J. Quant. Chem.*, 1994, **28**, 231.
42 J. P. Perdew and M. Levy, *Phys. Rev. B*, 1997, **56**, 16021.
43 R. A. King and N. C. Handy, *Phys. Chem. Chem. Phys.*, 2000, **2**, 5049.
44 O. Gunnarsson and B. I. Lundqvist, *Phys. Rev. B*, 1976, **13**, 4274.
45 H. Englisch and R. Englisch, *Physica*, 1983, **121A**, 253.
46 T. Ziegler, A. Rauk and E. J. Baerends, *Theor. Chim. Acta.*, 1977, **43**, 261.
47 U. von Barth, *Phys. Rev. A*, 1979, **20**, 1693.
48 T. Ziegler, *Chem. Rev.*, 1991, **91**, 651.
49 T. H. Dunning Jr., *J. Chem. Phys.*, 1989, **90**, 1007.
50 R. A. Kendall, T. H. Dunning Jr. and R. J. Harrison, *J. Chem. Phys.*, 1992, **96**, 6796.
51 D. E. Woon and T. H. Dunning Jr., *J. Chem. Phys.*, 1993, **98**, 1358.
52 D. E. Woon and T. H. Dunning Jr., *J. Chem. Phys.*, 1994, **100**, 2975.
53 K. A. Peterson, *J. Chem. Phys.*, 2003, **119**, 11099.
54 C. Cárdenas, P. W. Ayers, F. D. Proft, D. J. Tozer and P. Geerlings, *Phys. Chem. Chem. Phys.*, 2011, **13**, 2285.
55 *Gaussian 09, Revision A.1, M. J. Frisch, G. W. Trucks, H. B. Schlegel, G. E. Scuseria, M. A. Robb, J. R. Cheeseman, G. Scalmani, V. Barone, B. Mennucci, G. A. Petersson, H. Nakatsuji, M. Caricato, X. Li, H. P. Hratchian, A. F. Izmaylov, J. Bloino, G. Zheng, J. L. Sonnenberg, M. Hada, M. Ehara, K. Toyota, R. Fukuda, J. Hasegawa, M. Ishida, T. Nakajima, Y. Honda, O. Kitao, H. Nakai, T. Vreven, J. A. Montgomery, Jr., J. E. Peralta, F. Ogliaro, M. Bearpark, J. J. Heyd, E. Brothers, K. N. Kudin, V. N. Staroverov, R. Kobayashi, J. Normand, K. Raghavachari, A. Rendell, J. C. Burant, S. S. Iyengar, J. Tomasi, M. Cossi, N. Rega, J. M. Millam, M. Klene, J. E. Knox, J. B. Cross, V. Bakken, C. Adamo, J. Jaramillo, R. Gomperts, R. E. Stratmann, O. Yazyev, A. J. Austin, R. Cammi, C. Pomelli, J. W. Ochterski, R. L. Martin, K. Morokuma, V. G. Zakrzewski, G. A. Voth, P. Salvador, J. J. Dannenberg, S. Dapprich, A. D. Daniels, . Farkas, J. B. Foresman, J. V. Ortiz, J. Cioslowski, and D. J. Fox, Gaussian, Inc., Wallingford CT, 2009.*
56 K. Aidas, C. Angeli, K. L. Bak, V. Bakken, R. Bast, L. Boman, O. Christiansen, R. Cimiraglia, S. Coriani, P. Dahle, E. K. Dalskov, U. Ekström, T. Enevoldsen, J. J. Eriksen, P. Ettenhuber, B. Fernández, L. Ferrighi, H. Fliegl, L. Frediani, K. Hald, A. Halkier, C. Hättig, H. Heiberg, T. Helgaker, A. C. Hennum, H. Hettema, E. Hjerteniæs, S. Høst, I.-M. Høyvik, M. F. Iozzi, B. Jansík, H. J. Å. Jensen, D. Jonsson, P. Jørgensen, J. Kauczor, S. Kirpekar, T. Kjærgaard, W. Klopper, S. Knecht, R. Kobayashi, H. Koch, J. Kongsted, A. Krapp, K. Kristensen, A. Ligabue, O. B. Lutnæs, J. I. Melo, K. V. Mikkelsen, R. H. Myhre, C. Neiss, C. B. Nielsen, P. Norman, J. Olsen, J. M. H. Olsen, A. Osted, M. J. Packer, F. Pawlowski, T. B. Pedersen, P. F. Provasi, S. Reine, Z. Rinkevicius, T. A. Ruden, K. Ruud, V. Rybkin, P. Sałek, C. C. M. Samson, A. Sánchez de Merás, T. Saue, S. P. A. Sauer, B. Schimmelpfennig, K. Sneskov, A. H. Steindal, K. O. Sylvester-Hvid, P. R. Taylor, A. M. Teale, E. I. Tellgren, D. P. Tew, A. J. Thorvaldsen, L. Thøgersen, O. Vahtras, M. A. Watson, D. J. D. Wilson, M. Ziolkowski and H. Åagren, *WIRES Comput. Mol. Sci.*, 2013, **doi:**

10.1002/wcms.1172,.

57 *Dalton, a molecular electronic structure program, Release Dalton2013.0 (2013), see http://daltonprogram.org/*.

58 R. G. Parr and W. Yang, *Density Functional Theory of Atoms and Molecules*, Oxford University Press, New York, 1989.

59 R. G. Parr and W. Yang, *Ann. Rev. Phys. Chem.*, 1995, **46**, 701.

60 W. Kohn, A. D. Becke and R. G. Parr, *J. Phys. Chem.*, 1996, **100**, 12974.

61 H. Chermette, *J. Comput. Chem.*, 1999, **20**, 129.

62 P. Geerlings, F. De Proft and W. Langenaeker, *Adv. Quant. Chem.*, 1999, **33**, 303.

63 P. Geerlings, F. De Proft and W. Langenaeker, *Chem. Rev.*, 2003, **103**, 1793.

64 P. W. Ayers, J. S. M. Anderson and L. J. Bartolotti, *Int. J. Quantum Chem.*, 2005, **101**, 520.

65 J. L. Gázquez, *J. Mex. Chem. Soc.*, 2008, **52**, 3.

66 P. Geerlings and F. De Proft, *Phys. Chem. Chem. Phys.*, 2008, **10**, 3028.

67 S. B. Liu, *Acta. Phys.-Chem. China*, 2009, **25**, 590.

68 *Electronegativity*, ed. K. D. Sen, Springer-Verlag, Berlin, 1987, vol. 66.

69 R. G. Parr, R. A. Donnelly, M. Levy and W. E. Palke, *J. Chem. Phys.*, 1978, **68**, 3801.

70 R. S. Mulliken, *J. Chem. Phys.*, 1934, **2**, 782.

71 R. G. Parr and R. G. Pearson, *J. Am. Chem. Soc.*, 1983, **105**, 7512.

72 R. G. Pearson, *J. Am. Chem. Soc.*, 1963, **85**, 3533.

73 R. G. Pearson, *Science*, 1966, **151**, 172.

74 R. G. Pearson, *Chemical Hardness*, Wiley, New York, 1997.